



ELSEVIER

Contents lists available at ScienceDirect

Global and Planetary Change

journal homepage: www.elsevier.com/locate/gloplacha

Research article

Global water availability under high-end climate change: A vulnerability based assessment

A.G. Koutroulis^{a,*}, L.V. Papadimitriou^b, M.G. Grillakis^a, I.K. Tsanis^a, R. Warren^c, R.A. Betts^{d,e}^a School of Environmental Engineering, Technical University of Crete, Chania GR73100, Greece^b School of Water, Energy and Environment, Cranfield University, Cranfield, Bedford MK43 0AL, UK^c Tyndall Centre for Climate Change Research, School of Environmental Sciences, University of East Anglia, Norwich, UK^d Global Systems Institute, University of Exeter, Laver Building, North Park Road, Exeter EX4 4QE, UK^e Met Office Hadley Centre, FitzRoy Road, Exeter EX1 3PB, UK

ARTICLE INFO

Keywords:

Water resources
Global climate impacts
Adaptation
Vulnerability

ABSTRACT

Global sustainability is intertwined with freshwater security. Emerging changes in global freshwater availability have been recently detected as a combined result of human interventions, natural variability and climate change. Expected future socio-economic and climatic changes will further impact freshwater resources. The quantification of the impacts is challenging due to the complexity of interdependencies between physical and socio-economic systems. This study demonstrates a vulnerability based assessment of global freshwater availability through a conceptual framework, considering transient hydro-climatic impacts of crossing specific warming levels (1.5 °C, 2 °C and 4 °C) and related socio-economic developments under high-end climate change (RCP8.5). We use high resolution climate scenarios and a global land surface model to develop indicators of exposure for 25,000 watersheds. We also exploit spatially explicit datasets to describe a range of adaptation options through sensitivity and adaptive capacity indicators according to the Shared Socioeconomic Pathways (SSPs). The combined dynamics of climate and socio-economic changes suggest that although there is important potential for adaptation to reduce freshwater vulnerability, climate change risks cannot be totally and uniformly eliminated. In many regions, socio-economic developments will have greater impact on water availability compared to climate induced changes. The number of people under increased freshwater vulnerability varies substantially depending on the level of global warming and the degree of socio-economic developments, from almost 1 billion people at 4 °C and SSP5 to almost 3 billion people at 4 °C and SSP3. Generally, it is concluded that larger adaptation efforts are required to address the risks associated with higher levels of warming of 4 °C compared to the lower levels of 1.5 °C or 2 °C. The watershed scale and country level aggregated results of this study can provide a valuable resource for decision makers to plan for climate change adaptation and mitigation actions.

1. Introduction

Freshwater availability is drastically changing worldwide due to natural variability and direct or indirect human impacts (Kummu et al., 2016; Rodell et al., 2018). Climate change is expected to increase freshwater competition between sectors within the 21st century (Flörke et al., 2018), especially if mitigation actions are not implemented to avoid the highest probable levels of warming (Gerten et al., 2013; Papadimitriou et al., 2016). The effects of changes in social and economic factors, such as population growth and water consumption, might be as important or even more important than climate change in affecting the hydrological cycle and increasing water scarcity risk (Haddeland et al., 2013; Jacob et al., 2018; Kummu et al., 2016;

Schewe et al., 2014; Veldkamp et al., 2016). Thus, to provide outcomes relevant to policy making needs under the combined challenges of climate and socio-economic change, studies of hydrological impacts need to consider the human influences on the environmental system (Veldkamp et al., 2017) and employ integrated approaches that couple hydrology to socio-economics (Liu et al., 2017).

Although anthropogenic pressures can deteriorate hydrological climate change impacts, under a good and well planned management framework, human water usage can serve as an adaptation tool to global environmental change (Mehran et al., 2017). With the Paris Agreement target of limiting global warming becoming increasingly more difficult to achieve, future climate is expected to follow the higher end climate change scenarios (Burke et al., 2018). These higher levels of

* Corresponding author.

E-mail address: aris@hydromech.gr (A.G. Koutroulis).<https://doi.org/10.1016/j.gloplacha.2019.01.013>

Received 10 August 2018; Received in revised form 21 January 2019; Accepted 26 January 2019

Available online 29 January 2019

0921-8181/ © 2019 Published by Elsevier B.V.

warming are associated with significantly increased risks (Betts et al., 2018; Gerten et al., 2013; Grillakis et al., 2016; Papadimitriou et al., 2016; Schleussner et al., 2015; Smith et al., 2018). The prospect of high risks challenges adaptation efforts and poses adaptation associated with higher levels of global warming at the forefront of climate resilience policy (Rosenzweig et al., 2017).

A challenge of climate change adaptation studies is bridging the gap between global and regional/local assessments, as to proceed to implementation of adaptation measures decision makers will need information at least at the national level (Krishnamurthy et al., 2014). Steps in this direction have, for example, been reported by Koutroulis et al. (2016), who explore climate impacts and adaptation options at the local scale by translating global scale socio-economic scenarios to locally relevant input, and Carrão et al. (2016), who move from the global to the sub-national level within their global scale drought risk assessment.

A concept that encompasses climate change impacts, socio-economic influences and adaptation options and can flexibly be implemented across different scales is vulnerability. Vulnerability is typically defined as a function of three components: exposure, sensitivity and adaptation capacity (Parry, 2007). Recent literature examples of climate change vulnerability based assessments can be found in Ofori et al. (2017), who conduct a vulnerability assessment of biodiversity, Richardson et al. (2018) and Krishnamurthy et al. (2014), who examine food security, and Koutroulis et al. (2018), who use a vulnerability based framework to assess freshwater availability under climate change in Europe.

The present study is based on a conceptual framework, similar to the one applied by Koutroulis et al. (2018) for the examination of changes in vulnerability of European freshwater under high end climate change, extended to the global scale. We consider the RCP8.5 as the most representative scenario for higher end levels of global warming. The RCP8.5 can be combined with alternative socio-economic assumptions expressed by the Shared Socioeconomic Pathways (SSPs) (Moss et al., 2010; van Vuuren et al., 2014). Different socio-economic developments considered in the corresponding trajectories (SSP2, SSP3 and SSP5) were employed for the description of different levels of adaptation. The SSP3 was selected as the scenario of the highest adaptation challenges (closely related to the “no adaptation option” of the current report) followed by SSP2 as the “middle of the road” corresponding to medium adaptation challenges, and finally SSP5 as the lowest adaptation challenges scenario. Impacts are projected for different levels of adaptation in order to examine the extent to which they can be reduced at each global warming level.

2. Materials and methods

2.1. The vulnerability framework

For the assessment of the global vulnerability to freshwater stress at different Global Warming Levels (GWLs), defined with respect to the preindustrial, we employed the vulnerability conceptualization similar to the IPCC AR4 (Parry, 2007). The Vulnerability is determined by three basic components: the exposure to climate change, the sensitivity, and the capacity to adapt. The calculations were performed at the spatial level of roughly 25,000 Highly Accurate Global Drainage Basins developed by Masutomi et al. (2009), and used for the development of the Aqueduct Water Risk Atlas Global Maps (Gassert et al., 2014). The concept of the vulnerability to climate change provides a qualitative assessment of risk rather than quantitative projections of impacts. The various physical and socio-economic information composed to calculate vulnerability were converted to a common qualitative scale after a decile normalization (Fekete, 2009). The indicators used to conceptualize vulnerability to freshwater stress are listed in Table 1.

After a weighting robustness analysis we concluded to a standard equal weighting applied to the sub-indices of the major components of

exposure, sensitivity and adaptive capacity. This standard equal weighting procedure was chosen to avoid the subjectivity of assigning different sets of indicator weights. The weights that were assigned to the indices are included in Table ESM1 (equal weights). Finally, the three components of vulnerability (V) are combined as follows:

$$V = E + S - AC \quad (1)$$

where E is for exposure, S for sensitivity and AC for adaptive capacity. Higher exposure and sensitivity results to increased vulnerability and the opposite for higher adaptive capacity. Methodological details on the vulnerability calculations are included in the accompanying supplementary file.

Changes in freshwater vulnerability are assessed as differences between temporal averages of 30-year time slices from transient simulations passing a specific GWL, and the baseline period, here defined as the 1981 to 2010.

2.2. Exposure

Mean runoff production simulated by the JULES model served as a first index of exposure to freshwater stress (Papadimitriou et al., 2016). JULES is a physically based land surface model, simulating different processes such as the hydrological and carbon cycles, the surface exchange of energy fluxes, vegetation and plant physiology and others (Best et al., 2011). JULES model also includes the important process of the plant physiological response to increasing CO₂, which result in reducing evapotranspiration and therefore influence the runoff response (Betts et al., 2015; Milly and Dunne, 2016; Swann et al., 2016). A more detailed description of the JULES model setup is given by Papadimitriou et al. (2017) and further details are included in the supporting information file. The driving climate datasets are the climate model realizations included in Table 2. The table also includes the level of the atmospheric concentration of CO₂ (according to RCP8.5) at the time of passing each GWL proving that our analysis accounts for a wide range of concentrations to avoid under/over-estimation in projected hydrological changes (Betts and McNeall, 2018). They constitute simulation outputs from two higher resolution Atmosphere Global Climate Models (AGCMs) EC-EARTH3-v3.1 and HadGEM3-A Global Atmosphere configuration 6.0 (GA6.0) (Ciavarella et al., 2018), with prescribed time varying sea-surface temperatures (SSTs) and sea-ice concentrations (SICs), (Wyser et al., 2016). Both models are transition versions of those currently being used for the upcoming CMIP6 experiments. The new higher resolution projections (30–60 km) are driven by different sea surface temperatures covering a wide spectrum of future SSTs and SICs. The added value of the increased resolution is the improved representation of the physical processes and extremes (Betts et al., 2018; Koutroulis, 2018). Climate simulations that did not reach the higher level of examined warming (+4 °C) by the end of the simulation period were excluded from this analysis. An exception had to be made for two ensemble members (EC-Earth-R4 and EC-Earth-R7), for which the end of the GWL of 4 °C time-slice exceeds the end of the simulation period by four and two years respectively. Thus, the GWL of 4 °C time-slices for EC-Earth-R4 and EC-Earth-R7 are comprised of 26 and 28 years respectively. Additionally to the mean flow, low flows can serve as a second index of exposure to freshwater stress (Prudhomme et al., 2011). Low flow is defined here as the lowest 10% of time (10th percentile) on a daily time scale over a 30 year period and changes in low flows conditions is an indicator towards future hydrological extremes (Papadimitriou et al., 2016).

Drought indicators describing the severity and duration of hydro-meteorological extremes can efficiently support the development of freshwater exposure indicators (Stagge et al., 2015). Two drought indices are used for the analysis of drought conditions. The first is the standardized precipitation index (SPI) (Mckee et al., 1993), which is widely used for monitoring and assessment of the meteorological drought conditions. The second index is the standardized runoff index

Table 1

Indicators and expressions of exposure, sensitivity and adaptive capacity of vulnerability to freshwater scarcity. (Indicators marked in bold [*population, GDP, Water demand and Human capital*] are employing various relevant socioeconomic pathways [SSP2, SSP3 and SSP5]).

	Indicator	Expressed by
Exposure	Water availability on average	Relative changes in mean annual runoff production
	Low flows	Relative changes in 10th percentile runoff production
Sensitivity	Duration and severity of extreme events relevant to water availability (short and long term droughts)	Change in duration of short and long term meteorological droughts – index based on Standardized precipitation Index (SPI) of 6 and 48 months temporal scale
	Population density	Number of people totally affected by freshwater stress
	Total withdrawal	Consumptive and non-consumptive use
Adaptive capacity	Total cropland area	Arable land and permanent crops
	Water Demand sectoral	Gridded dataset of water demand per sector
	Economic resources available to adapt	GDP per capita (PPP)
	Law enforcement	World Governance Indicators (WGI) – World Bank
	Human Capital	Percent of highly educated working population
	Groundwater Resources	Extent of productive aquifers and inland water bodies for freshwater storage
	Upstream storage	Water storage capacity available upstream of a location relative to the total water supply at that location.

(SRI) (Shukla and Wood, 2008), which follows the SPI concept and characterizes hydrological drought by employing modelled runoff. In this study we focus on meteorological (SPI) and hydrological (SRI) droughts of severe intensity (SPI & SRI < -1.5). We also account for non-stationarity of climate change impacts by using the versions of relative SPI and SRI as developed by Dubrovsky et al. (2009). We used two temporal scales of the relative drought indices. A 6-month period (SRI-6) was employed for the representation of short term events that mostly correspond to agricultural droughts and a 48-month period (SRI-48) was used to depict long term drought events that affect the storage of hydrological resources.

2.3. Sensitivity

Population density is a first indicator of sensitivity to freshwater stress. Highly populated areas are more prone to water scarcity (Cutter and Finch, 2008; Yohe and Tol, 2002). In this study spatially explicit population scenarios consistent with the SSPs (Jones and O'Neill, 2016) at the timing of each GWL were calculated at the drainage basin level. A second sensitivity indicator is the total water withdrawal that can be expressed as the combined information of evaporated or polluted water losses due to consumptive use and not due to consumed remaining water that is returning to natural water bodies (Shiklomanov and Rodda, 2004). Water demand served also as a dynamic sensitivity indicator in terms of varying by SSP indicator. Total water demand for the recent past and for the GWLs was estimated based on the gridded

projections of water demand for specific SSPs, developed by Hanasaki et al. (2013). Using national statistics from the AQUASTAT database and water demand projections by Shen et al. (2010), Hanasaki et al. (2013) developed a dataset of sectorial future water demand taking into account technological developments in the efficiency of water use. Finally, the total cropland area (including irrigated and rainfed crops) as described in the HYDE 3.2 database developed by Klein Goldewijk et al. (2017) served as a sensitivity indicator to freshwater shortage. The values of time-varying sensitivity metrics for any particular Global Warming Level depended on the time at which that GWL was reached by each individual simulation (Table 2).

2.4. Adaptive capacity

The adaptive capacity to climate induced freshwater stress is defined as the potential of the society to deal with water scarcity. The per capita GDP (PPP) was used to develop the first indicator for mapping the available economic resources that can be utilized for obtaining water security. The Global dataset of gridded GDP scenarios developed by Murakami and Yamagata (2016) was used for SSP3 and SSP2 while for SSP5 the national GDP information included in the IIASA database were used in combination, for the derivation of the gridded GDP. Two additional indicators were employed for the consideration of the institutional developments associated to adaptation measures towards freshwater security. The first is the ability of law enforcement, which is an indicator of the governmental efficiency to formulate and implement

Table 2

High-resolution climate simulations explored in each chapter of this report. The table also indicates the time of reaching global warming levels of 1.5, 2 and 4 °C in each bias corrected forcing from the high-resolution climate simulations, driven by different sea surface temperatures (SSTs) and sea ice concentrations (SICs). The level of the atmospheric concentration of CO₂ (RCP8.5) at the time of passing the corresponding Global Warming Levels (GWL) is also listed.

Atmospheric general circulation model (AGCM)	Model providing driving SSTs & SICs	GWL 1.5		GWL 2.0		GWL 4.0	
		Time of passing	CO ₂ (ppm)	Time of passing	CO ₂ (ppm)	Time of passing	CO ₂ (ppm)
EC-EARTH3-v3.1	IPSL-CM5A-LR	2025	431.5	2036	472.0	2074	708.9
	GFDL-ESM2M	2038	480.5	2054	564.3	n/a	n/a
	HadGEM2-ES	2021	418.8	2035	467.9	2075	717.0
	EC-EARTH	2028	441.7	2043	503.5	2090	844.8
	GISS-E2-H	2031	452.5	2047	523.9	n/a	n/a
	IPSL-CM5A-LR	2024	428.2	2038	480.5	2072	692.9
	HadCM3LC	2026	434.8	2040	489.4	2088	827.2
HadGEM3-GA6.0	IPSL-CM5A-LR	2024	428.2	2035	467.9	2071	685.0
	GFDL-ESM2M	2036	472.0	2051	546.3	n/a	n/a
	HadGEM2-ES	2019	412.8	2033	460.0	2071	685.0
	IPSL-CM5A-MR	2023	425.0	2036	472.0	2069	669.3
	MIROC-ESM-CHEM	2020	415.8	2032	456.2	2068	661.6
	ACCESS1-0	2026	434.8	2040	489.4	2081	766.6

sound policies and regulations promoting private sector developments (Kaufmann et al., 2010). The underlying dataset is the Worldwide Governance Indicators (WGI) developed by the World Bank. Moreover, the human capital, expressed by the level of educational attainment was also considered as an adaptive capacity indicator, in the context of the societal capacity to elaborate and reconcile with policies related to water security. This indicator is the percent of highly educated workforce as derived by the Global Human Capital Data Sheet 2015, produced by the World Population Program (POP) including projections for level of educational attainment for all SSPs. The water storage potential is also an appropriate proxy of adaptive capacity, expressing the capacity to store water for use during a water shortage. The combined information from two indicators was used. The first was developed based on aquifer productivity and recharge potential data from the World-wide Hydrogeological Mapping and Assessment Programme (WHYMAP) for the major groundwater basins of the world. The second is related to artificial upstream storage potential as derived based on the global reservoir and dam database (Lehner et al., 2011). The values of time-varying adaptive capacity metrics for any particular Global Warming Level depended on the time at which that GWL was reached by each individual simulation (Table 2).

2.5. Adaptation challenges – scenarios

In our approach adaptation is expressed by the effect of development pathways and socio-economic changes, as they reflect on the developed vulnerability framework. Different degrees of adaptation are associated to the level of socio-economic challenges for adaptation as described by the IPCC scenario set (O'Neill et al., 2015). Three SSPs whose narrative is consistent to the RCP8.5 high end scenario were selected. SSP3-RCP8.5 is a scenario with high challenges for adaptation that can be closely compared to a “no adaptation option”. SSP2-RCP8.5 is forming a scenario of medium challenges for adaptation followed by the SSP5-RCP8.5 combination of low adaptation challenges. This information is fed into the vulnerability model through specific indicators based on detailed socio-economic projections for the 21st century according to the SSPs framework. The indicators used in this study are (a) the population density, (b) the total water demand, (c) the Gross Domestic Product (GDP) and (d) the human capital.

2.6. Robustness analysis

In order to test the robustness of the vulnerability assessment methodology, six different weightings were assigned to the different vulnerability dimensions (additional information on the weights is included in Table ESM1 of the supplementary file). The first set (W1) used an equal weighting scheme for all the indicators of each dimension. The next four weighting sets (W2–W5) apply increased (double) weight to each individual exposure or sensitivity indicator, while the last set of weights (W6) was adjusted to reflect the importance of the SSP varying indicators by applying higher weights to these indicators. In the case of adaptive capacity, the set W2 was chosen to reflect the importance of the physically based indicators related to water storage, the set W3 to reflect the sensitivity to economic factors (GDP) and the set W4 to reflect the importance of the social factors. The sets W5 and W6 are used to highlight the sensitivity of the resulting vulnerability to the SSP varying indicators as formulated in the present assessment. The six sets of weights were combined in a full factorial test for the three vulnerability dimensions, providing 216 ($6 \times 6 \times 6$) weighting combinations. The results of the robustness analysis are presented in Fig. 1. The figure presents the 216 weight combinations of the vulnerability for 40 out of the 221 examined countries. The illustrated countries were selected from the list of ranked vulnerability results, to represent the full range of vulnerability within the results. The average interquartile range is 10 ranks while the average range is 33 ranks from the total of 221 examined countries. The figure also shows the variability of the indicators

of exposure, sensitivity, adaptive capacity for the corresponding countries. The indicators of adaptive capacity and exposure exhibit similar variability to the resulting vulnerability with average interquartile range of 10 and 9 ranks, respectively, from the total of 221 examined countries. Sensitivity indicator has the lower variability with average interquartile range of 5 ranks suggesting a relatively stronger correlation between indicators such as total withdrawal and total cropland area. The results are considered to be robust enough as individual features and less robust as ranking outcome that is in fact expected given the nature of the vulnerability index and the interrelation of the sub-indices. The most robust results were obtained for Afghanistan, Mexico, and China while Bangladesh, Congo and Brazil show the wider range.

In order to further assess the robustness of the framework we compare the calculated vulnerability against results of weighted aggregates of water related risk and vulnerability schemes existing in the literature, the Water Risk Index (WRI) (Gassert et al., 2014; Reig et al., 2013) and the Human Development Index (HDI) (UNDP, 2013). These datasets have been used for the evaluation of the performance of similar schemes that examine water related vulnerability and risk (Carrão et al., 2016; Döll, 2009; Naumann et al., 2014). The WRI is a composite product of water related single indicators. These indicators are product of quantitative and qualitative datasets related to physical and regulatory water risks. The HDI is also developed from single socio-economic indicators and can serve as a proxy of vulnerability. The comparison is performed by means of a correlation analysis between the calculated vulnerability and (a) the WRI values per sub-basin fine scale level and per country level aggregated results and (b) the HDI values available at country level. Figure ESM1 of the Supplementary material illustrate the comparison of our model output with the WRI index. At the basin scale the range of the vulnerability is high, overlapping the classification of the WRI index. However, there is an increasing trend of the mean vulnerability with the increase in the severity of the WRI index. A similar behavior can be observed for the country level estimates. The opposite sign is apparent from the comparison between the country scale vulnerability and the Human Development Index, meaning that vulnerability is decreasing for higher levels of human development (Figure ESM2).

3. Results

3.1. Pathways of development

According to the SSP3 scenario and roughly half an additional degree compared to present warming following the RCP8.5 warming rate, global population is expected to increase by 7% ($\pm 8\%$), while at the levels of GWL2 and GWL4 an increase by +20% ($\pm 17\%$) and +53% ($\pm 10\%$), respectively, is foreseen. The average projected changes of population at country level (depending on the timing of each GWL reached by each driving model that is listed in Table 2) are illustrated for each SSP in Figure ESM3 of the supplemental file. The largest population increase is expected for the Middle East, East and West African and South Asian countries. In comparison to the SSP3 scenario (defined as the scenario with the highest adaptation challenges), population increase is expected to be less for the rest of the other two plausible socio-economic scenarios, SSP5 and SSP2. According to SSP2, 2%, 7% and 30% less population is expected for the warming levels of +1.5 °C, +2 °C + 4 °C, respectively, compared to SSP3, indicating lower sensitivity to freshwater stress. Further less population increase is associated to SSP5, mostly for the least and less developed countries and for the countries in transition. Only for the countries with advanced economies population is projected to increase according to the assumptions of the SSP5 (that considers lower levels of adaptation challenges).

Water demand scenarios reflect changes to irrigation extent and efficiency, crop intensity, as well as industrial and domestic water use. Extensive increase in water use is anticipated for all SSPs that is

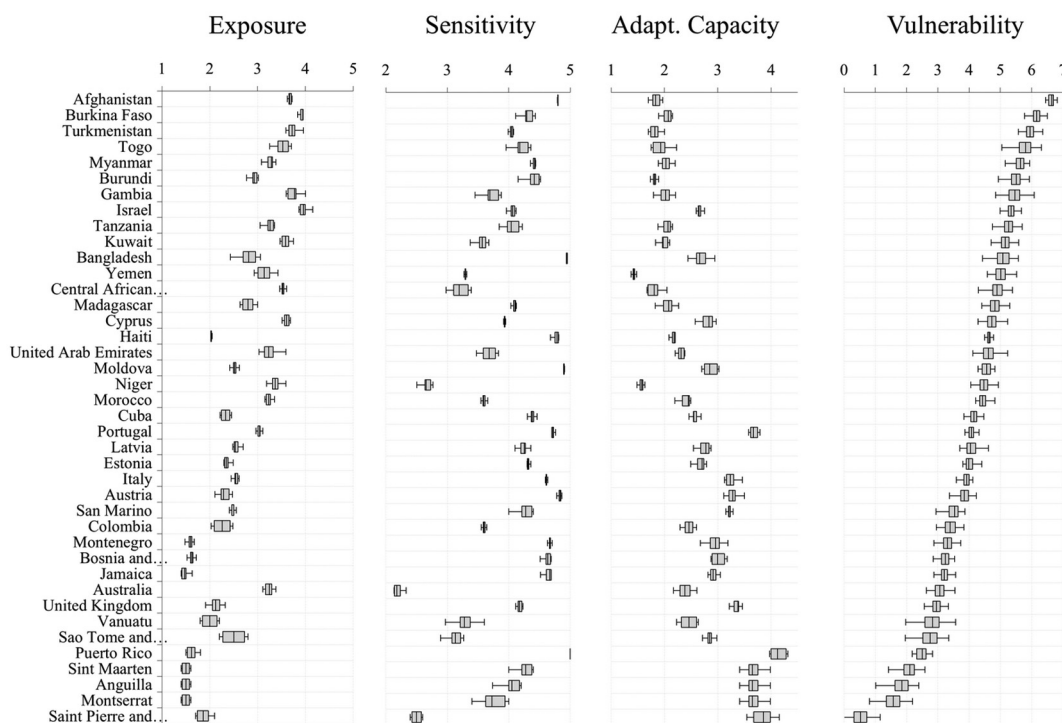


Fig. 1. Robustness analysis for exposure, sensitivity, adaptive capacity, and resulting vulnerability for 40 out of the 221 examined countries. The selection of the countries listed in the figure aiming for a full coverage of the range of the results. Countries are ranked based on their median vulnerability on a descending order. The horizontal axis denotes the value of the indicator, calculated at the basin level and aggregated at the country level.

exacerbated with the increase of warming (with time). According to SSP3 global water use can be increased by 59% (± 13%) at GWL1.5, by 75% (± 29%) at GWL2 and by 164% (± 19%) at GWL4 (Figure ESM4). Only European countries (Denmark, Ireland, Lithuania, Germany and others) are projected to have decreased water demand compared to the baseline period. Increased water use leads to higher sensitivity to freshwater stress. SSP2 is associated to less water demand by 33%, 39% and 85% for GWLs of 1.5 °C, 2 °C and 4 °C, respectively. This is due to the lower levels of growth in irrigated area and crop intensity of SSP2, as well as the higher water use efficiency mainly associated to irrigation technology. Only for specific countries like Cyprus, Czech Republic, Sweden and others (mostly European and Canada), water use is assumed to increase compared to SSP3. A similar picture of less water use, but more limited, is associated to SSP5. This is attributed to similar growth rates of irrigation area and crop intensity but higher water use efficiency.

Changes in GDP are projected to be more pronounced and highly differentiated among the three SSPs. Global GDP according to SSP3 is projected to increase by +236% (± 80%) by the time reaching the GWL1.5 on average, compared to the GDP of the year 2005. Increase is projected to +340% (± 101%) at the GWL2 warming level while at GWL4 could be as high as +534% (± 66%). Regarding the SSP2 that can be considered as a “business as usual” scenario an even greater GDP increase is assumed by +265% at the GWL1.5, +430% at the GWL2 and + 924% at the GWL4. As for the rapid economic development SSP5 scenario high rates of GDP increase are foreseen leading to a world with higher ability to adapt to high end climate change (Figure ESM5).

The final indicator that was used to describe the level of adaptation challenges is the evolution of human capital (Figure ESM6). Based on a ranking from 0 to 5 the global average human capital is projected to grow negligibly (by 0.1) according to SSP3, regardless the warming level, as a result of a pathway of stalled social development. The assumption of a fragmented world according to SSP3 portrays a regional diversity increasing with the level of warming (with time) depicting different rates of development (or depletion). Under the medium

challenges scenario (SSP2) the continuation of current development trends result to a significant higher level of human capital with less regional variation. According to the conventional development scenario (SSP5) the rates of human capital development are increased expecting to lead to an increase by +0.5 for the GWL1.5, +1.0 for the GWL2 and + 2.1 for the GWL4.

3.2. Impacts on freshwater vulnerability

Projected changes of exposure to freshwater availability as expressed by the relative scores in mean annual runoff production at the watershed level (Figure ESM9) show a highly patchy spatial pattern for the lower GWLs (1.5 °C and 2 °C). For the GWL4 the changes amplify and form more consistent spatial patterns of increased or decreased exposure. Higher exposure is projected for river basins around the Mediterranean region, the western Amazon, Central America, Central North America and South Africa. The increased exposure projected at the GWL2 for the northern Australian basins is shifted to lower exposure at the GWL4. Low flow has different response to warming resulting to different exposure changes. Higher exposure is foreseen for several basins over the tropical and subtropical zones at the GWL1.5 except subpolar zones and areas over central Asia. At the GWL2 increase in exposure is mitigated for northern America and decrease in low flow exposure is intensified over the northern latitudes. At the higher GWL4 low flow changes extended more towards increases (reduced exposure) except the wider Mediterranean region and South Equatorial Africa which are persistent to higher exposure. The shift of reduced exposure at GWL4 from increased exposure at GWL2 over Australia is also expected for low flows, only in this case the shift is apparent for the wider eastern Indian Ocean areas including South Asia and Southeast Asia.

The changes in exposure to short and long term meteorological droughts as calculated based on the new high resolution climate projections are illustrated in Figure ESM10. The Mediterranean region, the Amazon, Central and Central North America, Western South America,

Southeast Asia, Australia and South Africa regions are expected to face increased exposure in short term meteorological drought. Changes to the opposite direction are simulated for northern latitude and East Asia regions. Changes in exposure are intensified with global warming. Stronger increases and decreases are projected to long term (SPI48) than to short term (SPI6) droughts for the same regions. Hydrological droughts of the same temporal extent have been simulated using the JULES model (Figure ESM11). The spatial patterns of hydrological drought are less consistent compared to the corresponding of the meteorological drought due to the complex hydrological land surface interactions. Mediterranean and the Amazon are expected to be the most exposed regions to short term (SRI6) hydrological droughts (ignoring changes over the Sahara for which small changes are exaggerated due to the already dry state). For long term (SRI48) hydrological drought the spatial patterns are more consistent. South Africa and Central North America are added to the Mediterranean and Amazon hotspots of increasing exposure. The drying signal for several Australian and Southeast Asia basins at GWLs of 1.5 and 2 is shifted at the GWL4 (as depicted in the mean and low flow indicators).

The overall exposure resulting from the aforementioned sub-indices, for the baseline period and the GWLs, along with the exposure range within the different ensemble members and the changes compared to the baseline period are presented in Fig. 2. This figure shows country level aggregates of exposure, covering the global domain. At the baseline period, the most exposed regions are South Africa countries (Zambia, Zimbabwe, Botswana, Angola, Zambia), Mongolia and the wide Central East Asia, Russia and Canada. At GWL1.5, exposure is projected to increase over around 32% of the land surface. Increased

exposure is encountered for central North America, Brazil, regions of Europe and Africa, Southeast Asia and Australia, affecting around 38% of the global population. At +2 °C and +4 °C of warming, 30% and 26% of the land surface respectively is affected by increased exposure.

A note should be made here regarding the percent of land area affected by increased/decreased exposure and also sensitivity and adaptive capacity. The land fraction values stated in the text are derived from basin level spatial information. Meanwhile, the figures shown here present country level aggregates of the basin level information. Thus, the calculated fraction of land area under increased/decreased vulnerability components may not directly correspond to the area affected shown in the respective figure.

Country level aggregates of calculated sensitivity for the baseline period and changes per SSP and warming level are shown in Fig. 3. The maps show ensemble mean values, with the ensemble variation in sensitivity arising from the different times of passing each GWL in the different climate simulations (Table 2). This overall sensitivity is composed by four sub-indices from which the two are already described in Section 3.1 (Pathways of development) and are related to specific socio-economic developments in demographics (Figure ESM3) and water use and efficiency (Figure ESM4). Figure ESM12 illustrate the additional sensitivity indicators of total withdrawals related to consumptive and non-consumptive use and the total cropland area expressed by the total arable land and permanent crops. For all the examined SSPs, overall sensitivity increases with the level of warming, both in terms of the land fraction under increased sensitivity and affected population. For example, for SSP3, the fraction of land surface (and fraction of global population respectively) affected by increased sensitivity rises from

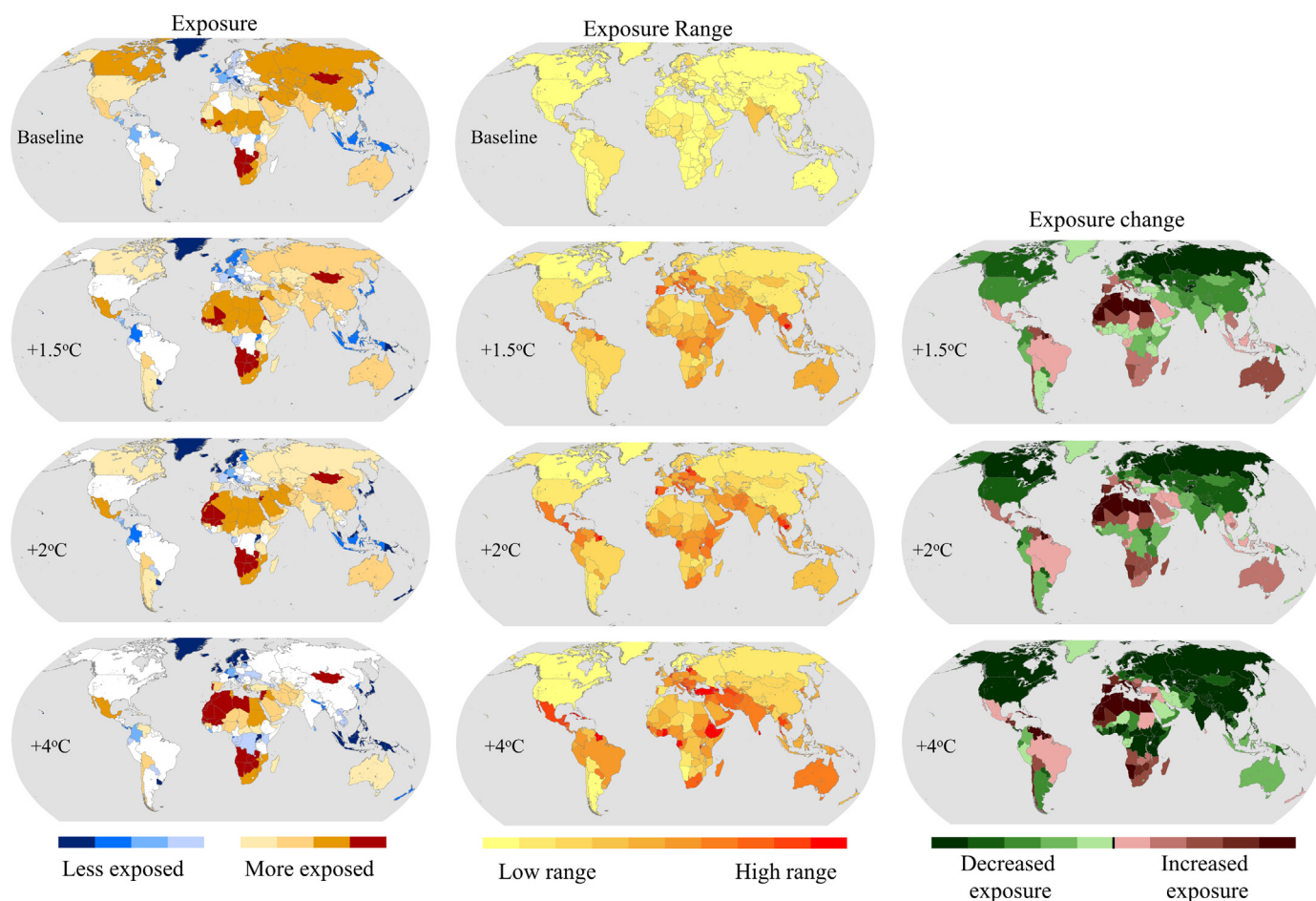


Fig. 2. Country level aggregated exposure representing the ensemble mean (left), exposure range between the ensemble members (middle) and exposure change per level of warming (right), compared to the baseline, at 1.5 °C, 2 °C and 4 °C of global warming.

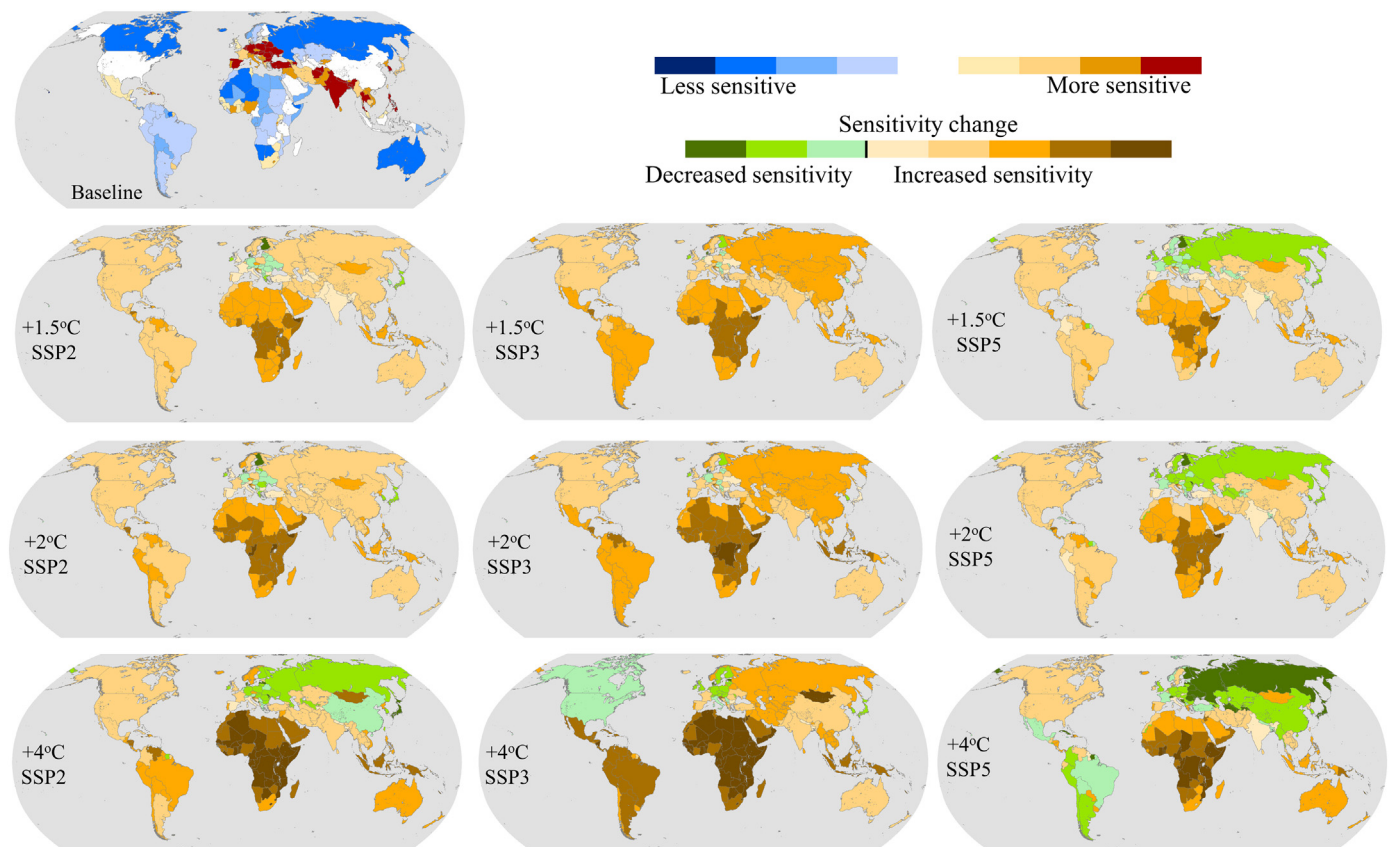


Fig. 3. Country level aggregated sensitivity of the baseline period (top panel), and changes in sensitivity per level of warming (1.5 °C, 2 °C and 4 °C) according to SSP2 (left), SSP3 (middle) and SSP5 (right). The sensitivity values shown represent the ensemble mean.

25% (16%) at GWL1.5 to 41% (30%) at GWL4. SSP3, as the scenario with the highest challenges for adaptation, shows the largest increase in sensitivity, compared to the other two SSPs. SSP5 shows the largest fraction of the land surface where decreased sensitivity is projected (13% at GWL4), followed by SSP2 (3% at GWL4). A respective ranking stands for the population affected by increased sensitivity, with SSP5 showing the smallest number of the three scenarios (20% of global population affected by increased sensitivity at GWL4), followed by SSP2 (26% at GWL4).

Country level information on the changes in adaptive capacity per SSP and warming level are shown in Fig. 4. The maps show ensemble mean values, with the ensemble variation in adaptive capacity arising from the different times of passing each GWL in the different climate simulations (Table 2). The overall adaptive capacity is composed by five sub-indices from which two are variable depending on the SSP. They are related to specific scenarios of economic development (Figure ESM5) and educational attainment (Figure ESM6) as described in Section 3.1. The rest of the sub-indices complementing adaptive capacity are (a) the law enforcement ability, (b) the extend of productive aquifers and inland water bodies for freshwater storage and (c) the water storage capacity available upstream of a location relative to the total water supply at that location, as shown in Figure ESM12. The overall adaptive capacity increases for the vast majority of the land surface regardless the SSP, with the increase intensifying as the level of warming increases (as the higher warming level corresponds to a time-period further in the future). Although the differences between the SSPs are very subtle, calculations of land fraction affected by increased adaptive capacity reveal that SSP3 exhibits the lowest adaptive capacity in terms of this metric (increased adaptive capacity over 91% of the land surface for SSP3, compared to 99% for SSP2 and SSP5).

The integration of the three vulnerability components (exposure, sensitivity and adaptive capacity) results in the final assessment of

vulnerability, which is presented in Fig. 5. For the baseline period, the most vulnerable countries are mainly located in the African and Asian continents. A general observation regarding vulnerability changes, is that vulnerability decreases for most countries. However, the Mediterranean, regions of Africa, Brazil, and Australia (for some SSP and warming level combinations) exhibit increases in freshwater vulnerability. SSP3, the socio-economic scenario resembling “no-adaptation”, shows a greater fraction of the land surface affected by increased vulnerability compared to SSP2 and SSP5 (25% for SSP3, compared to 18% and 10% for SSP2 and SSP5 respectively, all referring to GWL4 of warming). A respective ranking stands for the population affected by increased vulnerability, with SSP3 showing the largest fraction of global population affected by increased vulnerability (26% at GWL4), followed by SSP2 (18% at GWL4) and SSP5 (12% at GWL4). An interesting finding is that, for the same SSP, a smaller fraction of the land surface and the global population experience increased vulnerability at higher global warming levels. This behavior could be attributed to the temporal evolution (in terms of year of crossing a specific GWL) of the increased adaptive capacity at higher levels of warming, the decreased sensitivity due to increased water use efficiency further in the future and finally the reduced exposure projected for many regions under 4 °C of warming. However, this finding should be interpreted with caution, as the range of the uncertainty in the projections is higher at GWL4, as it can be observed from the exposure projections in Fig. 2.

For most countries freshwater vulnerability is foreseen to decrease (Fig. 5) as a combined effect of less exposure and/or lower sensitivity and/or higher adaptive capacity. There are also several countries, especially over the wider Mediterranean region, that are projected to face increased vulnerability regardless the level of adaptation and the level of warming. This is mostly driven by increased future exposure (Fig. 2), higher sensitivity (especially for the southern Mediterranean countries) and the low margin of adaptation potential (mostly for the

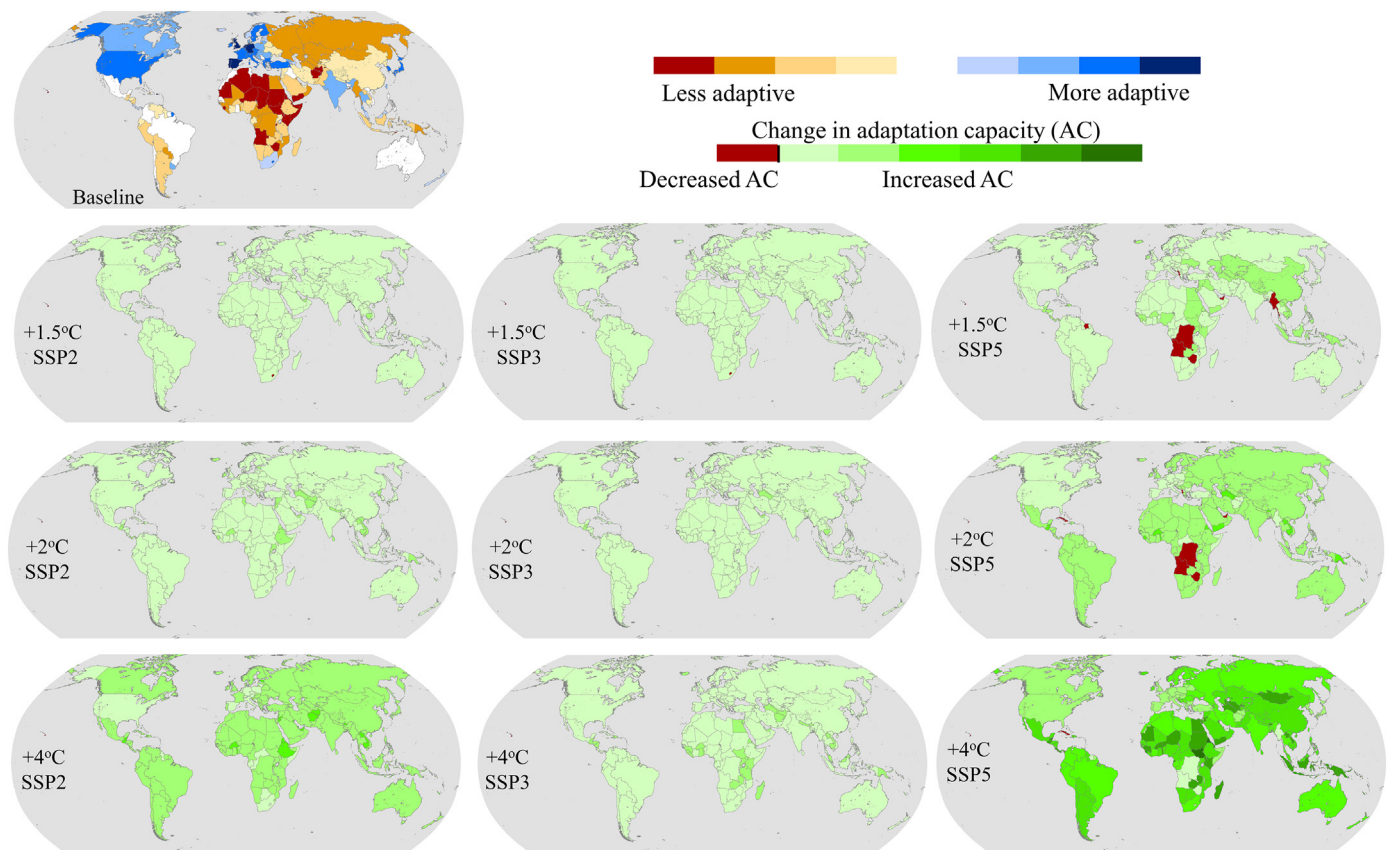


Fig. 4. Country level aggregated adaptive capacity of the baseline period (top panel), and changes in adaptive capacity per level of warming (1.5 °C, 2 °C and 4 °C) according to SSP2 (left), SSP3 (middle) and SSP5 (right). The adaptive capacity values shown represent the ensemble mean.

north Mediterranean countries).

3.3. Avoided impacts

We are using two metrics for reporting the impacts of climate change and level of adaptation at the global scale. The first is the number of people under increased vulnerability to water resources stress and the second is the fraction of global land area under the same assumption. It should be noted that the present analysis is based on spatially explicit population assumptions and thus the global size of population depends on the spatial distribution of population during the period of crossing the GWL for each model listed in Table 2 and according to the associated SSP.

Fig. 6 illustrates the changes in global population and land fraction affected by increased vulnerability to freshwater stress due to climate change (absolute values of changes). These global mean (across GCMs) projected changes at the GWL of 1.5 °C, 2 °C and 4 °C for different levels of adaptation are also included in Table ESM2 of the supplemental file. Despite the globally overall decreased exposure, more people (about 0.2 billion) are expected to face higher vulnerability solely for the SSP3 scenario at the warming level of +4 °C. The number of people affected by increased vulnerability under the SSP3 scenario is expected to be similar, on average (across all runs), for the +1.5 °C and +2 °C levels of warming. The fraction of global land area under increased vulnerability is decreasing with the increase of global temperature to varying degrees depending on the level of adaptation (SSPs). Particularly for the SSP3 scenario, the concurrent increase of affected population within a smaller area denotes a condensation of people to areas with increased vulnerability (relevant to the fast urbanization assumption of the SSP5 narrative). The level of adaptation assumed by the different narratives has a direct effect as described in the two metrics and illustrated in Fig. 6. Almost 2 billion people less are foreseen to face higher

freshwater vulnerability at GWL4 as a difference between the higher (SSP3) and lower (SSP5) adaptation challenges scenarios. Similar patterns of less affected people and smaller land area fraction are projected with the increase of adaptation level (moving from SSP3 to SSP2 and SSP5) and the increase of global warming.

Assuming a warming level of +4 °C combined with a future of high challenges to adaptation (SSP3) we can estimate the “avoided impacts” in terms of mitigation (by comparing the level of warming) and adaptation (comparing the level of adaptation assumed by SSP2 and SSP5). Fig. 7 (and Table ESM3) describe the global mean % impacts avoided relative to the GWL4-SSP3 (worst case scenario) for the GWLs of 1.5 °C, 2 °C and 4 °C and for different levels of adaptation. It has to be noted, once again, that warming is associated over time in the future and in parallel with the evolution of population according to the SSP. For example the global population assumed by the SSP3 narrative is approximately 11 billions at the GWL4 while for SSP2 and SSP5 is estimated to roughly 9 and 8 billions, respectively. These differences in projected population are estimated smaller for reduced levels of global warming (8.8 bn for SSP3, 8.3 bn for SSP2 and 8.0 bn for SSP5 at the GWL2). Limiting global warming to +2 °C or +1.5 °C following the SSP3-RCP8.5 scenario could result to negative impacts (larger extent of increased vulnerability by 6% at the GWL1.5 and by 3% at the GWL2) compared to the +4 °C state. This will also result to 7% less people at the GWL1.5 and 8% less at the GWL2 under increased vulnerability, but bearing in mind that global population (for SSP3) at the GWL1.5 (and the GWL2) is 28% (and 19%) less compared to the GWL4.

The impact of the different development pathways and socio-economic changes associated to the SSP narratives is evident in Fig. 7. Taking into account the evolution of population through the GWLs (time), according to the “medium adaptation scenario” (SSP2) 17%, 28% and 44% more people could avoid increased freshwater vulnerability at GWLs of 1.5 °C, 2 °C and 4 °C, respectively, compared to the

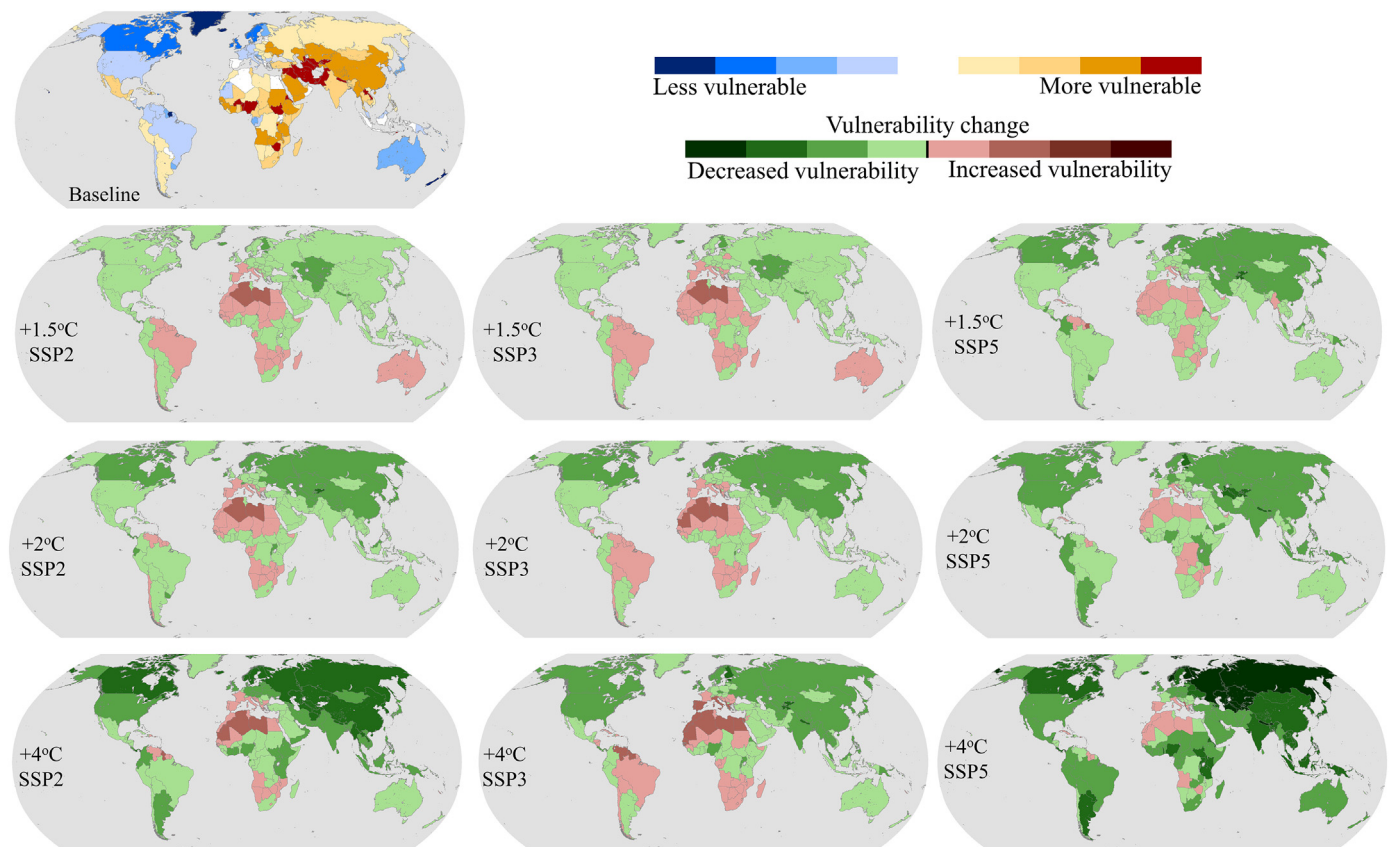


Fig. 5. Country level aggregated vulnerability of the baseline period (top panel), and changes in vulnerability per level of warming (1.5 °C, 2 °C and 4 °C) according to SSP2 (left), SSP3 (middle) and SSP5 (right). The vulnerability values shown represent the ensemble mean. The average year of crossing the 1.5 °C GWL between the ensemble members is 2025 (ranging from 2019 to 2038), 2038 (2032–2054) for the 2 °C GWL and 2073 (2068–2090) for the 4 °C GWL.

“worst case” SSP3-GWL4 scenario. At the GWLs of 1.5 °C and 2 °C, the benefit of SSP2 overcomes the differences from uneven population increase rates between SSP3 and SSP2. This is also depicted in the reduced (by 0.3% at GWL2 and by 8% at GWL4) land fraction with increased vulnerability to freshwater stress. The amelioration of increasing vulnerability is stronger for the SSP5 scenario. Especially comparing at the same level of global warming (+4 °C) and the same level of exposure, a 7% of global land area for SSP2 and 15% for SSP5 could avoid an increase in freshwater vulnerability as a result of socio-economic and technological developments (improved water efficiency, higher GDP and human capital). This could have a direct impact of avoiding higher freshwater vulnerability for 44% and 67% more people according to SSP2 and SSP5, respectively.

4. Discussion and conclusions

Here we present a conceptual framework for the assessment of the global freshwater vulnerability to high end climate change. Different socio-economic developments expressed by SSPs (SSP2, SSP3 and SSP5) are included in the framework to account for adaptation. SSP3 serves as the “no adaptation option”, while SSP2 is associated to medium adaptation challenges, and SSP5 to the lowest adaptation challenges. The climate change impacts on freshwater vulnerability are reported for different levels of adaptation and warming levels, to indicate the extent to which negative effects can be avoided by alternative adaptation approaches and lower levels of warming.

The presented framework provides a simple and transparent method for the assessment of vulnerability, taking into account not only the climate change impacts but further considering the socio-economic developments. An advantage of the present study is the use of data driven information of the highest available spatial detail for global

analysis, including state of the art in climate modeling, trying to model the best possible details. Moreover, the results are extracted at the basin level (calculated for 25,000 basins worldwide), which gives the added benefit of providing spatially detailed assessment of vulnerability, in a scale particularly useful for policy makers. The basin- and country- level results of this study can provide a valuable resource for decision makers to plan for climate change adaptation and mitigation actions. However, results at the local scale should be interpreted considering the modeling limitations and accounting for the climate and socio-economic scenario uncertainty which has been demonstrated and quantified by this study. It also has to be noted that the choice of SSPs of this study was primarily related to the GWL4. As the patterns of warming according to other RCPs for lower GWLs (1.5 °C and 2 °C) could be similar to RCP8.5, additional SSPs can be examined using this methodology.

Our new hydro-climatic projections suggest reduced exposure to freshwater stress for the northern regions and increases in exposure for subtropical regions but with a large range of responses, consistent with the findings by Greve et al. (2018). Despite the fact that the largest part of the land surface is foreseen to be less exposed to freshwater stress (and this exposure is reduced with global warming) there is still a large share of the global population that is projected to experience increased vulnerability, including many of the world's poorer regions. Comparing the findings of our analysis with earlier studies, Gerten et al. (2013) suggest an increase of 4%, 8% and 10% of the global population exposed to increased water scarcity under 1.5 °C, 2 °C, 3 °C global warming, respectively, considering a constant population. In contrast we find a reduction of the fraction of world's population with the increase of global warming as we consider future population changes and population is growing more (and/or less) in areas that become less (more) water stressed. Similar patterns of increasing water scarcity, but for higher portions of the global population (+8% for 1.5 °C, +14% for

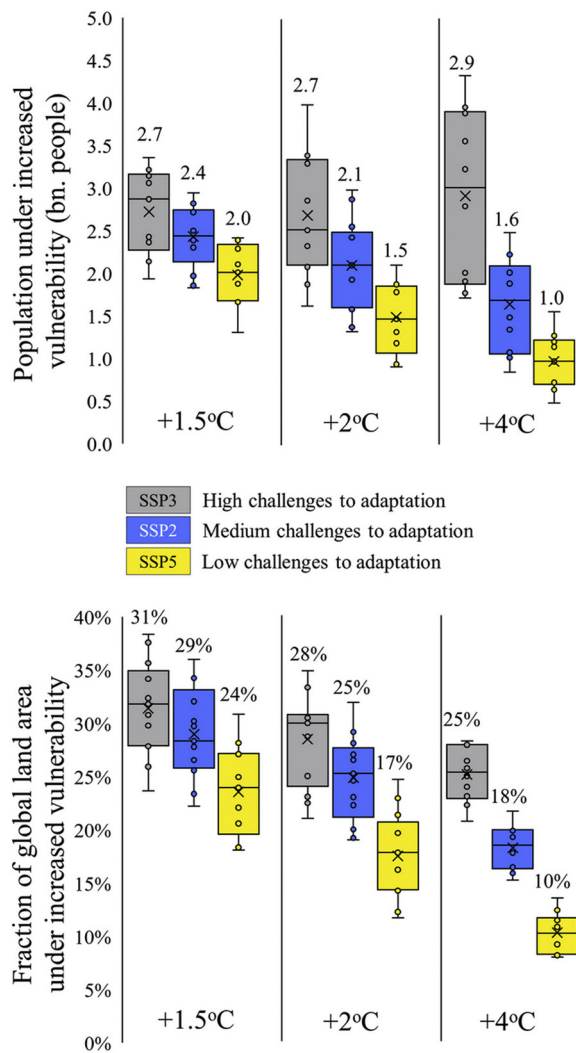


Fig. 6. Global mean (across GCMs) projected changes in global population and land fraction under increased vulnerability at 1.5 °C, 2 °C and 4 °C global warming for different levels of adaptation.

2 °C and + 17% for 3 °C of global warming) are projected by Schewe et al. (2014), assuming the RCP8.5 and the SSP2 population scenario. A more straightforward comparison can be performed with the results of the study by Arnell and Lloyd-Hughes (2014), in which they examine the exposure to freshwater stress, according to a set of climate and socio-economic scenarios. Despite the methodological differences (climate models, timing of global warming, definition of exposure metrics, population scenarios, etc.) our results on exposure and vulnerability are directly comparable following similar patterns of changes by the SSPs and the level of global warming (Table ESM4).

In many regions, socio-economic developments will have greater impact on water availability compared to climate induced changes, especially for the lower warming levels of 1.5 °C and 2 °C). Our results suggest that at 2 °C global warming (RCP8.5) and a “no adaptation” scenario (SSP3) nearly 2.7 billion people are foreseen to face increased vulnerability to freshwater stress. The “medium adaptation” scenario (SSP2) reduces the impacted population to 2.1 billion and the “high adaptation” (SSP5) to 1.5 billion people. At the 4 °C global warming and SSP3, 200 million more people could experience increased vulnerability (compared to 2 °C). For the 4 °C warming level and SSP2 roughly 1.65 billion people are expected to be more vulnerable (0.45 billion less than the 2 °C warming), while at the 4 °C and SSP5 this number is shaped to 1 billion (0.5 billion less than the 2 °C warming), due to the decrease or

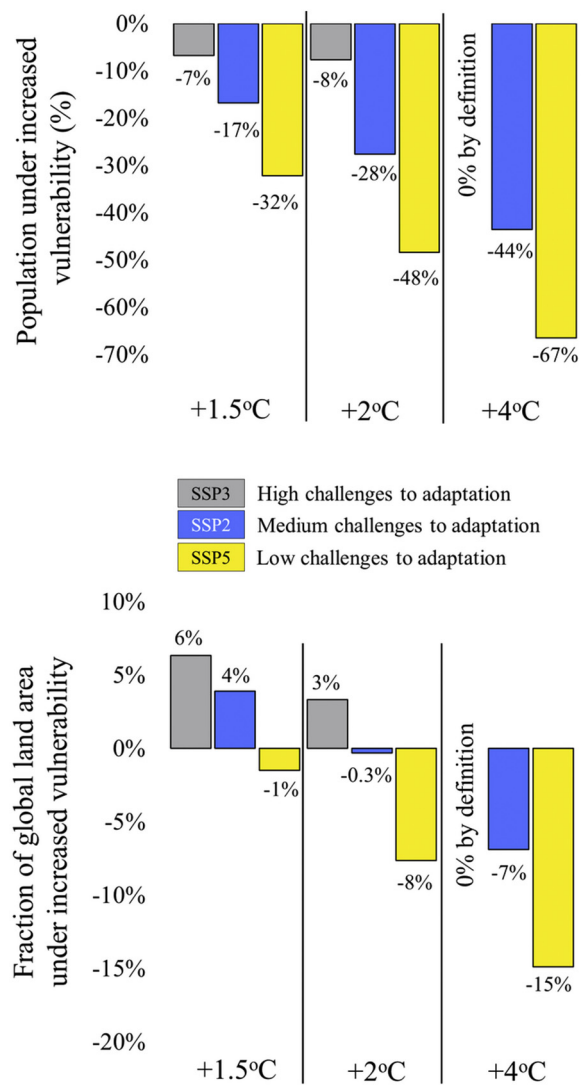


Fig. 7. Global mean (across GCM) % impacts avoided relative to 4 °C high adaptation challenges case (at 1.5 °C, 2 °C and 4 °C global warming and for different levels of adaptation). Negative values correspond to benefits (positive avoided impacts) and positive values correspond to disbenefits (negative avoided impacts) compared to the GWL4-SSP3 scenario.

the stabilization of the global population and the increase in adaptation capacity as a combination of less water demand, more economic resources available to adapt and higher human capital. The changes of affected population are driven by hydrological impacts but mainly by the spatial distribution and rates of population evolution as formulated in the shared socio-economic scenarios. Given that the relevant metric is the size of population with higher water stress, the abovementioned results are driven to a large extent by the fact that the population is growing more in the areas that become less water stressed, and/or less in the areas that become more water stressed.

This study indicates that, although there is important potential for adaptation to reduce freshwater vulnerability, climate change risks cannot be totally and uniformly eliminated. Generally, it is concluded that larger adaptation efforts are required to address the risks associated with higher levels of warming of 4 °C compared to the lower levels of 1.5 °C or 2 °C. In planning adaptation actions for the water sector, it should be considered that adaptation efficacy will also depend on interactions from other sectors, which might manifest as synergies or trade-offs. However, the explicit consideration of such sectorial feedbacks is out of the scope of the present study. Finally, especially for

adaptation relevant investments, there are a series of uncertainties that should be considered and quantified, from the uncertainties to the extent of adaptation needed to minimize or neutralize impacts, to uncertainties in future levels of warming and projections of regional climate and its associated impacts.

Authors' contribution

A.G.K. performed background research and designed the study with input from R.W., I.K.T. and R.A.B. Global land surface modeling was performed by L.V.P. and M.G.G. contributed to the development of the indicators. A.G.K. and L.V.P. wrote the manuscript. All authors discussed the results and commented on the manuscript.

Conflict of interest

The authors declare no competing interests.

Acknowledgements

The research leading to these results has received funding from the European Union Seventh Framework Programme FP7/2007-2013 under grant agreement no 603864 (HELIX: High-End CLimate Impacts and eXtremes; www.helixclimate.eu). We also thank John Caesar at the Met Office Hadley Centre for setting up and running the HadGEM3-GA6.0 simulations and also Klaus Wyser Strandberg and Shiyu Wang at the SMHI for setting up and running the EC-EARTH3 model v3. The EC-EARTH3-v3.1 simulations were performed on resources provided by the Swedish National Infrastructure for Computing (SNIC) at PDC and the HadGEM3-GA6.0 simulations were performed at the Met Office Hadley Centre. The work of R.A.B. was also supported by the Met Office Hadley Centre Climate Programme funded by BEIS and Defra. Kostantinos Seiradakis is finally acknowledged for his technical support on bias correction and JULES model setup.

Appendix A. Supplementary data

Supplementary data to this article can be found online at <https://doi.org/10.1016/j.gloplacha.2019.01.013>.

References

- Arnell, N.W., Lloyd-Hughes, B., 2014. The global-scale impacts of climate change on water resources and flooding under new climate and socio-economic scenarios. *Clim. Chang.* 122, 127–140. <https://doi.org/10.1007/s10584-013-0948-4>.
- Best, M.J., Pryor, M., Clark, D.B., Rooney, G.G., Essery, R.L.H., Ménard, C.B., Edwards, J.M., Hendry, M.a., Porson, a., Gedney, N., Mercado, L.M., Sitch, S., Blyth, E., Boucher, O., Cox, P.M., Grimmond, C.S.B., Harding, R.J., 2011. The Joint UK Land Environment Simulator (JULES), model description – part 1: energy and water fluxes. *Geosci. Model Dev.* 4, 677–699. <https://doi.org/10.5194/gmd-4-677-2011>.
- Betts, R.A., McNeill, D., 2018. How much CO₂ at 1.5 °C and 2 °C? *Nat. Clim. Chang.* 8, 546–548. <https://doi.org/10.1038/s41558-018-0199-5>.
- Betts, R.A., Golding, N., Gonzalez, P., Gornall, J., Kahana, R., Kay, G., Mitchell, L., Wiltshire, A., 2015. Climate and land use change impacts on global terrestrial ecosystems and river flows in the HadGEM2-ES Earth System Model using the Representative Concentration Pathways. *Biogeosci. Discuss.* 10, 6171–6223. <https://doi.org/10.5194/bg-12-1317-2015>.
- Betts, R.A., Bradshaw, C., Caesar, J., Friedlingstein, P., Gohar, L., Koutroulis, A., Lewis, K., Morfopoulos, C., Papadimitriou, L., Richardson, K., Tsanis, I., Wyser, K., 2018. Changes in climate extremes, river flows and vulnerability to food insecurity projected at 1.5 °C and 2 °C global warming with a higher-resolution global climate model. *Philos. Trans. R. Soc. A Math. Phys. Eng. Sci.* <https://doi.org/10.1098/rsta.2016.0452>.
- Burke, K.D., Williams, J.W., Chandler, M.A., Haywood, A.M., Lunt, D.J., Otto-Bliesner, B.L., 2018. Pliocene and Eocene provide best analogs for near-future climates. *Proc. Natl. Acad. Sci.* <https://doi.org/10.1073/PNAS.1809600115>. 201809600.
- Carrão, H., Naumann, G., Barbosa, P., 2016. Mapping global patterns of drought risk: an empirical framework based on sub-national estimates of hazard, exposure and vulnerability. *Glob. Environ. Chang.* 39, 108–124. <https://doi.org/10.1016/j.gloenvcha.2016.04.012>.
- Ciavarella, A., Christidis, N., Andrews, M., Groenendijk, M., Rostron, J., Elkington, M., Burke, C., Lott, F.C., Stott, P.A., 2018. Upgrade of the HadGEM3-a based attribution system to high resolution and a new validation framework for probabilistic event attribution. *Weather Clim. Extrem.* 20, 9–32. <https://doi.org/10.1016/J.WACE.2018.03.003>.
- Cutter, S.L., Finch, C., 2008. Temporal and spatial changes in social vulnerability to natural hazards. *Proc. Natl. Acad. Sci.* 105, 2301–2306. <https://doi.org/10.1073/pnas.0710375105>.
- Döll, P., 2009. Vulnerability to the impact of climate change on renewable groundwater resources: a global-scale assessment. *Environ. Res. Lett.* 4, 035006. <https://doi.org/10.1088/1748-9326/4/3/035006>.
- Dubrovsky, M., Svoboda, M.D., Trnka, M., Hayes, M.J., Wilhite, D.A., Zalud, Z., Hlavinka, P., 2009. Application of relative drought indices in assessing climate-change impacts on drought conditions in Czechia. *Theor. Appl. Climatol.* 96, 155–171. <https://doi.org/10.1007/s00704-008-0020-x>.
- Fekete, A., 2009. Validation of a social vulnerability index in context to river-floods in Germany. *Nat. Hazards Earth Syst. Sci.* 9, 393–403. <https://doi.org/10.5194/nhess-9-393-2009>.
- Flörke, M., Schneider, C., McDonald, R.I., 2018. Water competition between cities and agriculture driven by climate change and urban growth. *Nat. Sustain.* 1, 51–58. <https://doi.org/10.1038/s41893-017-0006-8>.
- Gassert, F., Luck, M., Landis, M., Reig, P., Shiao, T., 2014. Aqueduct global maps 2.1: constructing decision-relevant global water risk indicators. *World Resour. Inst.* https://www.wri.org/sites/default/files/Aqueduct_Global_Maps_2.1.pdf (20 pages).
- Gerten, D., Lucht, W., Ostberg, S., Heinke, J., Kowarsch, M., Kreft, H., Kundzewicz, Z.W., Rastgooy, J., Warren, R., Schellnhuber, H.J., 2013. Asynchronous exposure to global warming: freshwater resources and terrestrial ecosystems. *Environ. Res. Lett.* 8. <https://doi.org/10.1088/1748-9326/8/3/034032>.
- Greve, P., Gudmundsson, L., Seneviratne, S.I., 2018. Regional scaling of annual mean precipitation and water availability with global temperature change. *Earth Syst. Dyn.* 9, 227–240. <https://doi.org/10.5194/esd-9-227-2018>.
- Grillakis, M.G., Koutroulis, A.G., Papadimitriou, L.V., Daliakopoulos, I.N., Tsanis, I.K., 2016. Climate-induced shifts in global soil temperature regimes. *Soil Sci.* 181, 264–272. <https://doi.org/10.1097/SS.0000000000000156>.
- Haddeland, I., Heinke, J., Biemans, H., Eisner, S., Flörke, M., Hanasaki, N., Konzmann, M., Ludwig, F., Masaki, Y., Schewe, J., Stacke, T., Tessler, Z.D., Wada, Y., Wisser, D., 2013. Global water resources affected by human interventions and climate change. *Proc. Natl. Acad. Sci.* 111, 3251–3256. <https://doi.org/10.1073/pnas.1222475110>.
- Hanasaki, N., Fujimori, S., Yamamoto, T., Yoshikawa, S., Masaki, Y., Hijioka, Y., Kainuma, M., Kanamori, Y., Masui, T., Takahashi, K., Kanae, S., 2013. A global water scarcity assessment under Shared Socio-economic Pathways – Part 1: water use. *Hydrol. Earth Syst. Sci.* 17, 2375–2391. <https://doi.org/10.5194/hess-17-2375-2013>.
- Jacob, D., Kotova, L., Teichmann, C., Sobolowski, S.P., Vautard, R., Donnelly, C., Koutroulis, A.G., Grillakis, M.G., Tsanis, I.K., Damm, A., Sakalli, A., van Vliet, M.T.H., 2018. Climate impacts in Europe under +1.5°C global warming. *Earth's Futur.* 6. <https://doi.org/10.1002/2017EF000710>.
- Jones, B., O'Neill, B.C., 2016. Spatially explicit global population scenarios consistent with the Shared Socioeconomic Pathways. *Environ. Res. Lett.* 11, 084003. <https://doi.org/10.1088/1748-9326/11/8/084003>.
- Kaufmann, D., Kraay, A., Mastruzzi, M., 2010. *The Worldwide Governance Indicators: Methodology and Analytical Issues.* The World Bank.
- Klein Goldewijk, K., Beusen, A., Doelman, J., Stehfest, E., 2017. Anthropogenic land use estimates for the Holocene – HYDE 3.2. *Earth Syst. Sci. Data* 9, 927–953. <https://doi.org/10.5194/essd-9-927-2017>.
- Koutroulis, A.G., 2018. Dryland changes under different levels of global warming. *Sci. Total Environ.* <https://doi.org/10.1016/j.scitotenv.2018.11.215>.
- Koutroulis, A.G., Grillakis, M.G., Daliakopoulos, I.N., Tsanis, I.K., Jacob, D., 2016. Cross sectoral impacts on water availability at +2°C and +3°C for East Mediterranean island states: the case of Crete. *J. Hydrol.* 532. <https://doi.org/10.1016/j.jhydrol.2015.11.015>.
- Koutroulis, A.G., Papadimitriou, L.V., Grillakis, M.G., Tsanis, I.K., Wyser, K., Betts, R.A., 2018. Freshwater vulnerability under high end climate change. A pan-European assessment. *Sci. Total Environ.* 613–614. <https://doi.org/10.1016/j.scitotenv.2017.09.074>.
- Krishnamurthy, P.K., Lewis, K., Choularton, R.J., 2014. A methodological framework for rapidly assessing the impacts of climate risk on national-level food security through a vulnerability index. *Glob. Environ. Chang.* 25, 121–132. <https://doi.org/10.1016/j.gloenvcha.2013.11.004>.
- Kummu, M., Guillaume, J.H.A., De Moel, H., Eisner, S., Flörke, M., Porkka, M., Siebert, S., Veldkamp, T.I.E., Ward, P.J., 2016. The world's road to water scarcity: shortage and stress in the 20th century and pathways towards sustainability. *Sci. Rep.* 6, 1–16. <https://doi.org/10.1038/srep38495>.
- Lehner, B., Liermann, C.R., Revenga, C., Vörösmarty, C., Fekete, B., Crouzet, P., Döll, P., Endejan, M., Frenken, K., Magome, J., Nilsson, C., Robertson, J.C., Rödel, R., Sindorf, N., Wisser, D., 2011. High-resolution mapping of the world's reservoirs and dams for sustainable river-flow management. *Front. Ecol. Environ.* 9, 494–502. <https://doi.org/10.1890/100125>.
- Liu, J., Yang, H., Gosling, S.N., Kummu, M., Flörke, M., Hanasaki, N., Wada, Y., Zhang, X., Zheng, C., 2017. Water scarcity assessments in the past, present, and future. *Earth's Futur.* 5, 545–559. <https://doi.org/10.1002/ef2.200>.
- Masutomi, Y., Inui, Y., Takahashi, K., Matsuoka, Y., 2009. Development of highly accurate global polygonal drainage basin data. *Hydrol. Process.* 23, 572–584. <https://doi.org/10.1002/hyp.7186>.
- Mckee, T.B., Doesken, N.J., Kleist, J., 1993. The relationship of drought frequency and duration to time scales 17–22.
- Mehran, A., AghaKouchak, A., Nakhjiri, N., Stewardson, M.J., Peel, M.C., Phillips, T.J., Wada, Y., Ravalico, J.K., 2017. Compounding impacts of human-induced water stress and climate change on water availability. *Sci. Rep.* 7, 1–9. <https://doi.org/10.1038/>

- s41598-017-06765-0.
- Milly, P.C.D., Dunne, K.A., 2016. Potential evapotranspiration and continental drying. *Nat. Clim. Chang.* 6, 946–949. <https://doi.org/10.1038/nclimate3046>.
- Moss, R.H., Edmonds, J.A., Hibbard, K.A., Manning, M.R., Rose, S.K., van Vuuren, D.P., Carter, T.R., Emori, S., Kainuma, M., Kram, T., Meehl, G.A., Mitchell, J.F.B., Nakicenovic, N., Riahi, K., Smith, S.J., Stouffer, R.J., Thomson, A.M., Weyant, J.P., Wilbanks, T.J., 2010. The next generation of scenarios for climate change research and assessment. *Nature* 463, 747–756. <https://doi.org/10.1038/nature08823>.
- Murakami, D., Yamagata, Y., 2016. Estimation of Gridded Population and GDP Scenarios with Spatially Explicit Statistical Downscaling. (arXiv Prepr. arXiv1610.09041).
- Naumann, G., Barbosa, P., Garrote, L., Iglesias, A., Vogt, J., 2014. Exploring drought vulnerability in Africa: an indicator based analysis to be used in early warning systems. *Hydrol. Earth Syst. Sci.* 18, 1591–1604. <https://doi.org/10.5194/hess-18-1591-2014>.
- Ofori, B.Y., Stow, A.J., Baumgartner, J.B., Beaumont, L.J., 2017. Influence of adaptive capacity on the outcome of climate change vulnerability assessment. *Sci. Rep.* 7, 1–12. <https://doi.org/10.1038/s41598-017-13245-y>.
- O'Neill, B.C., Krieglner, E., Ebi, K.L., Kemp-Benedict, E., Riahi, K., Rothman, D.S., van Ruijven, B.J., van Vuuren, D.P., Birkmann, J., Kok, K., Levy, M., Solecki, W., 2015. The roads ahead: narratives for shared socioeconomic pathways describing world futures in the 21st century. *Glob. Environ. Chang.* <https://doi.org/10.1016/j.gloenvcha.2015.01.004>.
- Papadimitriou, L.V., Koutroulis, A.G., Grillakis, M.G., Tsanis, I.K., 2016. High-end climate change impact on European runoff and low flows – exploring the effects of forcing biases. *Hydrol. Earth Syst. Sci.* 20, 1785–1808. <https://doi.org/10.5194/hess-20-1785-2016>.
- Papadimitriou, L.V., Koutroulis, A.G., Grillakis, M.G., Tsanis, I.K., 2017. The effect of GCM biases on global runoff simulations of a land surface model. *Hydrol. Earth Syst. Sci.* 21, 4379–4401. <https://doi.org/10.5194/hess-21-4379-2017>.
- Parry, M.L., 2007. *Climate Change 2007: Impacts, Adaptation and Vulnerability: Contribution of Working Group II to the Fourth Assessment Report of the Intergovernmental Panel on Climate Change*. Cambridge University Press.
- Prudhomme, C., Parry, S., Hannaford, J., Clark, D.B., Hagemann, S., Voss, F., 2011. How well do large-scale models reproduce regional hydrological extremes in Europe? *J. Hydrometeorol.* 12, 1181–1204. <https://doi.org/10.1175/2011JHM1387.1>.
- Reig, P., Shiao, T., Gassert, F., 2013. *Aqueduct Water Risk Framework*. WRI Working Paper. World Resources Institute, forthcoming, Washington, DC.
- Richardson, K.J., Lewis, K.H., Krishnamurthy, P.K., Kent, C., Wiltshire, A.J., Hanlon, H.M., 2018. Food security outcomes under a changing climate: impacts of mitigation and adaptation on vulnerability to food insecurity. *Clim. Chang.* 147, 327–341. <https://doi.org/10.1007/s10584-018-2137-y>.
- Rodell, M., Famiglietti, J.S., Wiese, D.N., Reager, J.T., Beaudoin, H.K., Landerer, F.W., Lo, M.H., 2018. Emerging trends in global freshwater availability. *Nature*. <https://doi.org/10.1038/s41586-018-0123-1>.
- Rosenzweig, C., Arnell, N.W., Ebi, K.L., Otze-Campen, H., Raes, F., Rapley, C., Stafford Smith, M., Cramer, W., Frieler, K., Reyer, C.P.O., Schewe, J., van Vuuren, D., Warszawski, L., 2017. Assessing inter-sectoral climate change risks: the role of ISIMIP. *Assessing inter-sectoral climate change risks: the role of ISIMIP*. *Environ. Res. Lett.* 12. <https://doi.org/10.1088/1748-9326/12/1/010301>.
- Schewe, J., Heinke, J., Gerten, D., Haddeland, I., Arnell, N.W., Clark, D.B., Dankers, R., Eisner, S., Fekete, B.M., Colón-González, F.J., Gosling, S.N., Kim, H., Liu, X., Masaki, Y., Portmann, F.T., Satoh, Y., Stacke, T., Tang, Q., Wada, Y., Wisser, D., Albrecht, T., Frieler, K., Piontek, F., Warszawski, L., Kabat, P., 2014. Multimodel assessment of water scarcity under climate change. *Proc. Natl. Acad. Sci. U. S. A.* 111, 3245–3250. <https://doi.org/10.1073/pnas.1222460110>.
- Schleussner, C.-F., Lissner, T.K., Fischer, E.M., Wohland, J., Perrette, M., Golly, A., Rogelj, J., Childers, K., Schewe, J., Frieler, K., Mengel, M., Hare, W., Schaeffer, M., 2015. Differential climate impacts for policy-relevant limits to global warming: the case of 1.5 °C and 2 °C. *Earth Syst. Dyn. Discuss.* 6, 2447–2505. <https://doi.org/10.5194/esdd-6-2447-2015>.
- Shen, Y., Oki, T., Utsumi, N., Kanae, S., Hanasaki, N., 2010. Projection of future world water resources under SRES scenarios: water withdrawal/Projection des ressources en eau mondiales futures selon les scénarios du RSSE: prélèvement d'eau. *Hydrol. Sci. J.* 53, 11–33. <https://doi.org/10.1623/hysj.53.1.11>.
- Shiklomanov, I.A., Rodda, J.C., 2004. *World Water Resources at the Beginning of the Twenty-First Century*. Cambridge University Press.
- Shukla, S., Wood, A.W., 2008. Use of a standardized runoff index for characterizing hydrologic drought. *Geophys. Res. Lett.* 35. <https://doi.org/10.1029/2007GL032487>. L02405.
- Smith, P., Price, J., Molotoks, A., Malhi, Y., Soc, T.R., Smith, P., 2018. *Impacts on Terrestrial Biodiversity of Moving from a 2 °C to a 1.5 °C Target Subject Areas: Author for correspondence*.
- Stagge, J.H., Tallaksen, L.M., Gudmundsson, L., Van Loon, A.F., Stahl, K., 2015. Candidate distributions for climatological drought indices (SPI and SPEI). *Int. J. Climatol.* 35, 4027–4040. <https://doi.org/10.1002/joc.4267>.
- Swann, A.L.S., Hoffman, F.M., Koven, C.D., Randerson, J.T., 2016. Plant responses to increasing CO2 reduce estimates of climate impacts on drought severity. *Proc. Natl. Acad. Sci. U. S. A.* 113, 10019–10024. <https://doi.org/10.1073/pnas.1604581113>.
- UNDP, 2013. *The rise of the South: human progress in a diverse world*. Hum. Dev. Report. http://hdr.undp.org/sites/default/files/reports/14/hdr2013_en_complete.pdf (23 pages).
- van Vuuren, D.P., Krieglner, E., O'Neill, B.C., Ebi, K.L., Riahi, K., Carter, T.R., Edmonds, J., Hallegatte, S., Kram, T., Mathur, R., Winkler, H., 2014. A new scenario framework for climate Change Research: scenario matrix architecture. *Clim. Chang.* 122, 373–386. <https://doi.org/10.1007/s10584-013-0906-1>.
- Veldkamp, T.I.E., Wada, Y., Aerts, J.C.J.H., Ward, P.J., 2016. Towards a global water scarcity risk assessment framework: incorporation of probability distributions and hydro-climatic variability. *Environ. Res. Lett.* 11 (2), 024006.
- Veldkamp, T.I.E., Wada, Y., Aerts, J.C.J.H., Döll, P., Gosling, S.N., Liu, J., Masaki, Y., Oki, T., Ostberg, S., Pokhrel, Y., Satoh, Y., Kim, H., Ward, P.J., 2017. Water scarcity hotspots travel downstream due to human interventions in the 20th and 21st century. *Nat. Commun.* 8. <https://doi.org/10.1038/ncomms15697>.
- Wyser, K., Strandberg, G., Caesar, J., Gohar, L., 2016. *Documentation of Changes in Climate Variability and Extremes Simulated by the HELIX AGCMs at the 3 SWLs and Comparison in Equivalent SST/SIG Low-Resolution CMIP5. (HELIX project deliverable 3.1. projections)*.
- Yohe, G., Tol, R.S.J., 2002. Indicators for social and economic coping capacity – moving toward a working definition of adaptive capacity. *Glob. Environ. Chang.* 12, 25–40. [https://doi.org/10.1016/S0959-3780\(01\)00026-7](https://doi.org/10.1016/S0959-3780(01)00026-7).